Scattering from underground tunnels

1982 J. Phys. A: Math. Gen. 15 459

(http://iopscience.iop.org/0305-4470/15/2/018)

J. Phys. A: Math. Gen. **15** (1982) 459–471. Printed in Great Britain

Scattering from underground tunnels†

Nikolaos K Uzunoglu and J D Kanellopoulos

Department of Electrical Engineering, National Technical University of Athens, Athens 147, Greece

Received 5 March 1981, in final form 20 July 1981

Abstract. The scattering of electromagnetic waves from underground tunnels is investigated analytically. A Green function approach is employed to formulate the problem for horizontally polarised incident waves. This approach results in an integral equation for the unknown interior field $\boldsymbol{E}(r)$ for the buried scatterer region. Expansion of the unknown $\boldsymbol{E}(r)$ field in terms of cylindrical wavefunctions in conjunction with the basic integral equation leads to an infinite set of linear equations. An analytical procedure is developed to decouple this system of equations when the excessive phaseshift inside the scattering region is small. This determines the inner field $\boldsymbol{E}(r)$ of the scatterer. In order to compute the scattered field for the far-field region a steepest descent integration technique is employed. Numerical results are obtained for several cases and are presented.

1. Introduction

Detection and identification of underground inhomogeneities with electromagnetic probing methods is an area of current interest (Burrell and Peters 1979, Chan *et al* 1979). An interesting problem in this area is the identification of tunnels and underground pipes.

Several techniques are employed to obtain information for buried inhomogeneities such as the short video pulse method (Sullivan 1970), use of extremely low frequencies (Cauterman *et al* 1979), the transient response method (Mahmoud *et al* 1979, Lee 1979) and finally passive detection techniques by observing the anomalies of the geomagnetic field (Tikhonov 1950, Wait 1962). Apart from the attenuation of the waves, due to the finite conductivity of the soil, the very complex electromagnetic structure of the ground environment complicates the problem of the detection of the buried scatterers to a great extent. The former problem, i.e. the attenuation of echo signals, can be tackled by using higher transmission power levels, lower frequencies or signal processing techniques. The latter problem is much more complex because of the high clutter energy returning from the ground environment. Therefore, prior to any experiment, it is useful to have *a priori* quantitive information on the scattered field from possible underground targets. This requires a good knowledge of the interaction of electromagnetic waves impinging from the air with geological media.

In this paper, scattering from buried infinite cylinders is investigated analytically. The geometry of the problem is defined in figure 1 where D is the depth of the cylindrical scatterer axis from the earth surface, α is the cylinder radius and n_1, n_2 are the complex refractive indices for the ground and scatterer regions. The free space

† Partially supported by the Research Council of NTUA.

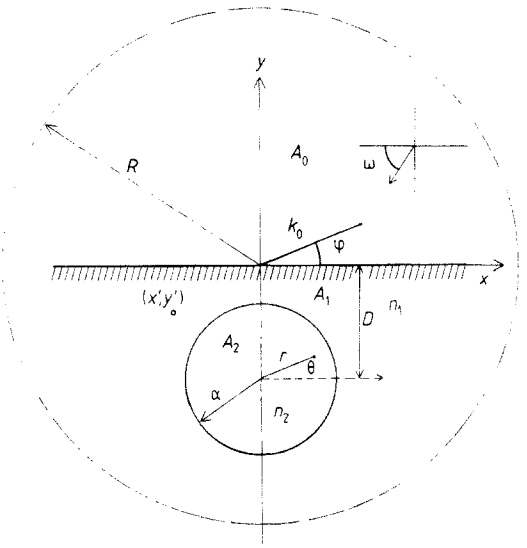

Figure 1. Geometry of the scattering from an underground cylindrical tunnel.

wavenumber for $y>0$ (air) is shown by k_0 and the whole space is assumed to be magnetically homogeneous with a magnetic permeability of the free space $\mu = \mu_0 = 4\pi \times 10^{-7}\,\mathrm{H\,m^{-1}}$.

An integral equation approach is used to formulate the corresponding boundary value problem for an electromagnetic plane wave impinging from the air. The incident wave direction is assumed to be perpendicular to the cylinder axis. In this paper only horizontally polarised waves are considered. Techniques similar to those of the present work can be employed to treat the case of vertically polarised waves. The analysis starts with the application of Green's theorem which results in an integral equation for the unknown interior electric field $\boldsymbol{E}(\boldsymbol{r})$ of the buried scattering region. Expansion of the unknown interior field $\boldsymbol{E}(\boldsymbol{r})$ in terms of the circular cylindrical wavefunctions and substitution of this into the integral equations results in an infinite set of coupled equations. In order to solve this system of equations, an approximate decoupling procedure is developed when $k_0\alpha|n_2-n_1|<1$. This determines the unknown field $\boldsymbol{E}(\boldsymbol{r})$ as a power series in $k_0\alpha(n_2-n_1)$. Finally the scattered field is computed in the air (for $y>0$) employing the method of steepest descent. Numerical results are obtained and presented for the upper band of high (HF) and very high (VHF) frequencies for several ground types (n_1 values), scatterer dimensions and refractive indices (n_2). In the following analysis the time dependence for the field is assumed to be $\exp(-\mathrm{i}2\pi ft)$ and is suppressed throughout the analysis.

2. Formulation of the mathematical problem

A Green function approach is employed to formulate the corresponding boundary value problem. To this end, the Green function in the absence of the ground scatterer (i.e. $n_2 = n_1$) is determined for a unit line source. Assuming the primary excitation to be located inside the earth ($y'<0$) the Green function is the solution of the equation

$$(\nabla^2 + k^2(\boldsymbol{r}))G(\boldsymbol{r}\,|\,\boldsymbol{r}') = -\delta(r-r') \tag{1}$$

where $\boldsymbol{r} = x\hat{x} + y\hat{y}$ and $\boldsymbol{r}' = x'\hat{x} + y'\hat{y}$ are the line source coordinates as shown in figure 1 and

$$k(\boldsymbol{r}) = \begin{cases} k_0 & \text{for } y > 0 \\ k_0 n_1 & \text{for } y < 0. \end{cases}$$

In addition to equation (1), as the Green function is the z component of the electric field, it should satisfy the appropriate boundary conditions on the earth–air interface at $y = 0$. To this end a method due to Sommerfeld (1949) is used as follows. Since the primary excitation is inside the ground ($y' < 0$) the total field $G(\boldsymbol{r}|\boldsymbol{r}')$ for the air and earth regions can be written as

$$G(\boldsymbol{r}|\boldsymbol{r}') = \begin{cases} G_0(\boldsymbol{r}) + G_1(\boldsymbol{r}) & y < 0 \\ G_2(\boldsymbol{r}) & y > 0 \end{cases} \tag{2}$$

where $G_0(\boldsymbol{r}) = \frac{1}{4}iH_0^{(1)}(k_1|\boldsymbol{r} - \boldsymbol{r}'|)$ is the free space (primary source) Green function where $k_1 = k_0 n_1$ and $H_0(x)$ is the zeroth-order cylindrical Hankel function. $G_1(\boldsymbol{r})$ and $G_2(\boldsymbol{r})$ are the induced electric fields for $y < 0$ and $y > 0$ respectively. Considering the solution of the wave equation (1) these are expressed as Fourier integrals

$$G_1(\boldsymbol{r}) = \langle e^{\mu_1 y} A(\lambda)/\mu_1 \rangle \qquad y < 0 \tag{3}$$

$$G_2(\boldsymbol{r}) = \langle e^{-\mu_0 y} B(\lambda)/\mu_1 \rangle \qquad y > 0 \tag{4}$$

where the bracket operator is defined as

$$\langle Q \rangle = \frac{1}{4\pi} \int_{-\infty}^{+\infty} d\lambda \, \exp[i\lambda(x - x')] Q(\lambda). \tag{5}$$

$\mu_j = (\lambda^2 - k_j^2)^{1/2}$ for $j = 0, 1$ and $A(\lambda)$, $B(\lambda)$ are unknown coefficients to be determined. Expressing the free space term as (Sommerfeld 1949)

$$G_0(\boldsymbol{r}) = \langle \exp(-\mu_1|y - y'|/\mu_1) \rangle \tag{6}$$

$$G_0(x\hat{x}) + G_1(x\hat{x}) = G_2(x\hat{x}) \tag{7}$$

$$\frac{\partial}{\partial y}(G_0(\boldsymbol{r}) + G_1(\boldsymbol{r}))|_{y=0} = \frac{\partial}{\partial y} G_2(\boldsymbol{r})|_{y=0}. \tag{8}$$

The secondary field coefficients are

$$A(\lambda) = \frac{\mu_1 - \mu_0}{\mu_1 + \mu_0} e^{\mu_1 y'} \qquad B(\lambda) = \frac{2\mu_1}{\mu_1 + \mu_0} e^{\mu_1 y'}. \tag{9}$$

Let us assume now that a plane wave is incident from the air on the earth's surface as shown in figure 1. The incident wavevector $\boldsymbol{k}_i = k_0(-\cos\omega\hat{x} - \sin\omega\hat{y})$ is assumed to be perpendicular to the z axis.

If no scatterer existed inside the earth, then the total field would be given in terms of the Fresnel coefficients as

$$\psi_0 = \begin{cases} \exp[-ik_0\rho\cos(\varphi - \omega)] + R_h \exp[-ik_0\rho\cos(\varphi + \omega)] & y > 0 \\ (1 + R_h)\exp[-ik_0 n_1 \rho\cos(\varphi - \omega')] & y < 0 \end{cases} \tag{10}$$

where

$$R_h = \frac{\sin\omega - \sqrt{n_1^2 - \cos^2\omega}}{\sin\omega + \sqrt{n_1^2 - \cos^2\omega}} \qquad \frac{\cos\omega'}{\cos\omega} = \frac{1}{n_1}.$$

$\rho = (x^2+y^2)^{1/2}$, $\varphi = \tan^{-1}(y/x)$ are the polar coordinates and ω is the angle between the $-y$ axis and incident direction. Since $n_1 = (\varepsilon_{r1} + i\sigma_1/\omega\varepsilon_0)^{1/2}$ is a complex quantity the angle ω' is also complex and is a function of the earth's relative dielectric constant ε_{r1} and conductivity σ_1.

If there is an inhomogeneity inside the earth then the field ψ_0 of equation (10) is distorted because of the excitation of secondary sources inside the scattering region. This distortion of the field can be expressed in a compact form using Green's theorem. Indeed, applying Green's theorem for a circle of radius ρ of figure 1, we have

$$\iint_{A\rho} [(\psi(\boldsymbol{r}') - \psi_0(\boldsymbol{r}'))\nabla'^2 G(\boldsymbol{r}|\boldsymbol{r}') - G(\boldsymbol{r}|\boldsymbol{r}')\nabla'^2(\psi(\boldsymbol{r}') - \psi_0(\boldsymbol{r}'))]\,\mathrm{d}\Omega'$$

$$= \int_{c_0} \left((\psi(\boldsymbol{r}) - \psi_0(\boldsymbol{r}))\frac{\partial G(\boldsymbol{r}|\boldsymbol{r}')}{\partial \rho} - G(\boldsymbol{r}|\boldsymbol{r}')\frac{\partial}{\partial \rho}(\psi(\boldsymbol{r}) - \psi_0(\boldsymbol{r})) \right) \mathrm{d}l \tag{11}$$

where $\mathrm{d}\Omega' = \mathrm{d}x'\,\mathrm{d}y'$, ψ is the total electric field, $A\rho = A_0 + A_1 + A_2$ is the area inside the circle and the contour c_0 is the corresponding circumference.

The fields $(\psi - \psi_0)$ and G originating from a finite scattering region and a line source should satisfy the Sommerfeld radiation conditions and both fields should decay as $1/\sqrt{\rho}$ as $\rho \to +\infty$ ($\rho = (x^2+y^2)^{1/2}$). Thus going to the limit $\rho \to +\infty$, the right-hand side of equation (11) vanishes. Substitution of the appropriate wave equations for ψ, ψ_0 and the functions $G(\boldsymbol{r}|\boldsymbol{r}')$ simplifies the left-hand side of equation (10) to

$$\psi(\boldsymbol{r}) = \psi_0(\boldsymbol{r}) + (k_2^2 - k_1^2) \iint_{A_2} G(\boldsymbol{r}|\boldsymbol{r}')\psi(\boldsymbol{r}')\,\mathrm{d}\Omega'. \tag{12}$$

In this equation the point $\boldsymbol{r}$ can be in any region (i.e. earth, scatterer or air). If the point $\boldsymbol{r}$ is restricted inside the inhomogeneity region A_2 then equation (12) is an integral equation for the unknown field $\psi(\boldsymbol{r})$. It should be noted here that the shape of the inhomogeneity region A_2 can be arbitrary although in the present treatment circular cross section scatterers only are considered.

3. Evaluation of the interior field

The inner field for the region A_2 can be expanded in terms of cylindrical wavefunctions as

$$\psi(\boldsymbol{r}) = \sum_{m'=-\infty}^{+\infty} C_{m'} J_{m'}(k_2 r)\, \mathrm{e}^{\mathrm{i}m'\theta} \tag{13}$$

where (r, θ) are the polar local coordinates (see figure 1) for the scattering region and are expressed in terms of the initial coordinates $\boldsymbol{r}$ as (see figure 1)

$$x = r\cos\theta \qquad y = -D + r\sin\theta. \tag{14}$$

Substituting equations (13) and (10) into equation (12) ($\boldsymbol{r} \in A_2$), multiplying both sides with $\exp(-\mathrm{i}m\theta)$ and integrating from $\theta = 0$ to 2π we obtain

$$2\pi C_m J_m(k_2 r) = (1 + R_h)\exp(\mathrm{i}k_1 D \sin\omega')$$

$$\times \int_0^{2\pi} \mathrm{d}\theta \exp[-\mathrm{i}m\theta - \mathrm{i}k_0 n_1 r\cos(\theta - \omega)]$$

$$+(k_2^2-k_1^2)\int_{\theta=0}^{2\pi}\mathrm{d}\theta\int_{r'=0}^{\alpha}r'\,\mathrm{d}r'\int_{\theta'=0}^{2\pi}\mathrm{d}\theta'\exp(-\mathrm{i}m\theta)$$

$$\times(G_0(\boldsymbol{r})+G_1(\boldsymbol{r}))\Big(\sum_{m'}C_{m'}J_{m'}(k_2r')\exp(\mathrm{i}m'\theta')\Big) \tag{15}$$

where

$$\sum_{m'}\equiv\sum_{m'=-\infty}^{+\infty}.$$

Introducing equations (3) and (9) for $G_1(\boldsymbol{r})$, and employing the well known expansion of the free space Green function in terms of cylindrical wavefunctions as

$$G_0(\boldsymbol{r})=\tfrac{1}{4}\mathrm{i}H_0(k_1|\boldsymbol{r}-\boldsymbol{r}'|)=\tfrac{1}{4}\mathrm{i}\sum_{n=-\infty}^{+\infty}J_n(k_1r_<)H_n(k_1r_>)\exp[\mathrm{i}n(\theta-\theta')] \tag{16}$$

with $r_<=\min(r,r')$ and $r_>=\max(r,r')$, equation (15) after the integrations over θ and θ' can be written as

$$C_mJ_m(k_2r)=(1+R_h)\exp[\mathrm{i}k_1D\sin\omega'-\mathrm{i}m(\tfrac{1}{2}\pi+\omega')]J_m(k_1r)$$

$$+(k_2^2-k_1^2)\tfrac{1}{2}\mathrm{i}\pi C_m\int_{r'=0}^{\alpha}r'\,\mathrm{d}r'\,J_m(k_1r_<)H_m(k_1r_>)J_m(k_2r')$$

$$+\tfrac{1}{2}(k_2^2-k_1^2)\int_{r'=0}^{\alpha}r'\,\mathrm{d}r'\sum_{m'}K_{mm'}C_{m'}J_m(k_1r)J_{m'}(k_1r')J_{m'}(k_2r') \tag{17}$$

where

$$K_{mm'}=\mathrm{i}^{m-m'}\int_C\mathrm{d}\lambda\,\frac{\exp(-2D\mu_1)}{\mu_1}\,\frac{\mu_1-\mu_0}{\mu_1+\mu_0}\exp[-\mathrm{i}(m+m')\theta_1] \tag{18}$$

$$\theta_1=\tan^{-1}(-\mathrm{i}\mu_1/\lambda) \tag{19}$$

and the contour C is shown in figure 2.

In the above integrations we use repeatedly the definite integral

$$\int_0^{2\pi}\mathrm{d}\theta\exp(-\mathrm{i}m\theta+\mu_1r\sin\theta+\mathrm{i}\lambda r\cos\theta)=2\pi\mathrm{i}^{-m}J_m(k_1r)\exp(-\mathrm{i}m\theta_1).$$

The integrals for r and r' are computed easily using the well known relations for Bessel functions (Abramowitz and Stegun 1965). After some straightforward algebra equation (17) reduces to

$$C_mK_m(X_1,X_2)-\sum_{m'}K_{mm'}C_{m'}L_{m'}(X_1,X_2)$$

$$=2(1+R_h)\exp[\mathrm{i}k_1D\sin\omega'-\mathrm{i}m(\tfrac{1}{2}\pi+\omega')] \tag{20}$$

where

$$X_1=k_1\alpha\qquad X_2=k_2\alpha$$

$$K_m(X_1,X_2)=\pi\mathrm{i}(X_1H_{m+1}(X_1)J_m(X_2)-X_2H_m(X_1)J_{m+1}(X_2))$$

$$L_m(X_1,X_2)=X_2J_{m+1}(X_2)J_m(X_1)-X_1J_{m+1}(X_1)J_m(X_2).$$

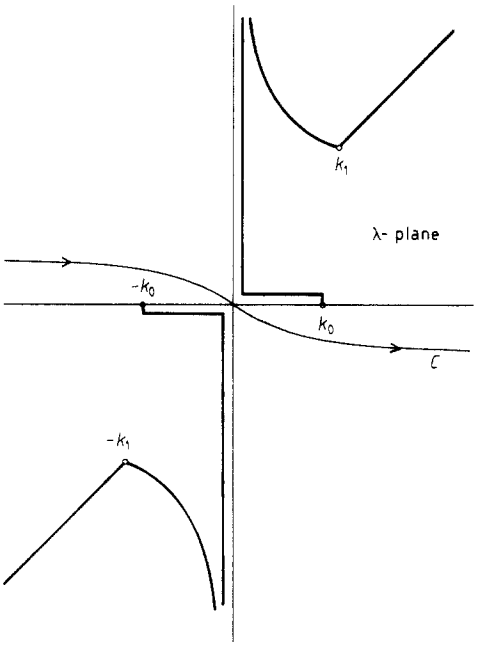

Figure 2. Complex λ plane for the integration in equation (18).

The set of equations of the form (20) for $-\infty < m < +\infty$ constitutes an infinite set of coupled equations which cannot be solved in general with existing mathematical techniques. Of course numerical techniques could be used to solve this system employing some truncation procedure to obtain a finite set of equations; instead we proceed using a Taylor expansion in $(X_2 - X_1)$

$$K_m(X_1, X_2) = K_m(0) + (X_2 - X_1)K_m(1) + (X_2 - X_1)^2 K_m(2) + \dots \tag{21}$$

with analogous expansions for L_m and C_m. Note that $K_m(0) = 2$ and $L_m(0) = 0$.

In the appendix the expressions for $K_m(i)$, $L_m(i)$ (i = 1, 2) are given. Introducing the expansions of $K_m(X_1, X_2)$, $L_m(X_1, X_2)$ and C_m into equation (20) and equating the terms of the same order, an iterative procedure is derived as

$$C_m(0) = (1 + R_h)\exp[ik_1 D \sin\omega' - im(\tfrac{1}{2}\pi + \omega')] \tag{22}$$

$$C_m(1) = -\tfrac{1}{2}C_m(0)K_m(1) + \tfrac{1}{2}\sum_{m'} K_{mm'}C_{m'}(0)L_{m'}(1) \tag{23}$$

$$C_m(2) = -\tfrac{1}{2}C_m(1)K_m(1) - \tfrac{1}{2}C_m(0)K_m(2) + \tfrac{1}{2}\sum_{m'} K_{mm'}(C_{m'}(0)L_{m'}(2) + C_{m'}(1)L_{m'}(1)). \tag{24}$$

It should be noted that this procedure is valid when $|X_2 - X_1| < 1$ since otherwise the expansions are slowly convergent. It is also necessary to compute the coupling integrals $K_{mm'}$ as defined in equation (18). A numerical integration procedure is developed to compute these integrals. The following key points need to be taken into account.

(i) In all of the above equations the square roots μ_1 and μ_0 should be defined appropriately so that the outgoing wave conditions (Collin 1960) for equations (3), (4)

and (6) are satisfied. This is achieved by choosing the appropriate branch cuts as described by Collin (1960) which are shown in figure 2. The branch cut for μ_1 are hyperbolae defined as $\mathrm{Re}(\lambda)\,\mathrm{Im}(\lambda) = \mathrm{Re}(k_1)\,\mathrm{Im}(k_1)$. Since $\mathrm{Im}(k_0) = 0$ the branch cut for μ_0 degenerates to a broken line as given in figure 2. The substitutions $z = \mu_1/\lambda$ and $W = (1+z)/(1-z)$ enable $\mathrm{i}\theta_1$ to be written from equation (19) as

$$\mathrm{i}\theta_1 = \tfrac{1}{2}\ln(W). \tag{25}$$

In figures 3(*a*), 3(*b*) and 3(*c*) the images of the contour C (figure 2) are shown for the z, W and $\mathrm{i}\theta_1$ complex planes respectively. It can be shown from figure 3(*c*) that an appropriate branch cut for the function $\mathrm{i}\theta_1$ is the real positive axis of the W plane. Evaluating the inverse transformations $W \to z$ and $z \to \lambda$, the branch cuts in the λ plane can be found to be straight lines originating from the points $\lambda = \pm k_1$ and going to infinity along the lines $\arg(\lambda) = 45°$ and $-135°$. Accordingly, the functions μ_1, μ_0 and $\mathrm{i}\theta_1$ are

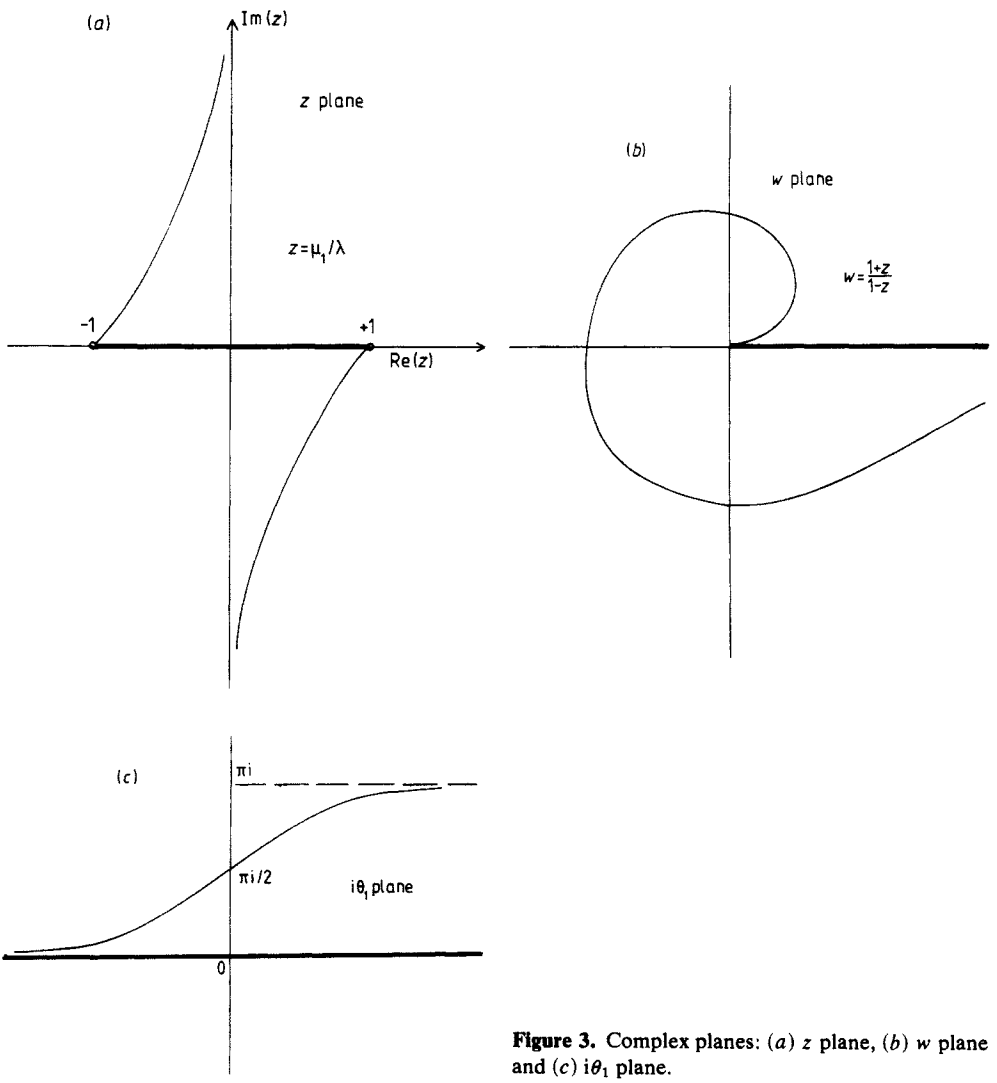

Figure 3. Complex planes: (*a*) z plane, (*b*) w plane and (*c*) $\mathrm{i}\theta_1$ plane.

defined exactly and the corresponding values on the contour C of the complex λ plane are

$$\mu_0 = \begin{cases} -\mathrm{i}(k_0^2 - \lambda^2)^{1/2} & |\lambda| < k_0 \\ (\lambda^2 - k_0^2)^{1/2} & |\lambda| > k_0 \end{cases} \tag{26}$$

$$\mu_1 = s\mathrm{e}^{\mathrm{i}a}$$

with

$$a = \begin{cases} \frac{1}{2}[\tan^{-1}(-\gamma_1) - \tan^{-1}(\gamma_2)] & -\infty < \lambda < -k_{ir} \\ \frac{1}{2}[\tan^{-1}(\gamma_1^{-1}) - \frac{1}{2}\pi - \tan^{-1}(\gamma_2)] & k_{ir} < \lambda < k_{ir} \\ \frac{1}{2}[-\tan^{-1}(\gamma_1) + \tan^{-1}(-\gamma_2)] & k_{ir} < \lambda < +\infty \end{cases} \tag{27}$$

$$s = \{[k_{1i}^2 + (\lambda - k_{1r})^2][k_{1i}^2 + (\lambda + k_{1r})^2]\}^{1/4} \qquad -\infty < \lambda < +\infty$$

$$\gamma_1 = \frac{k_{1r} + \lambda}{k_{1i}} \qquad \gamma_2 = \frac{k_{1r} - \lambda}{k_{1i}} \qquad k_1 = k_{1r} + \mathrm{i}k_{1i}$$

and finally

$$\mathrm{i}\theta_i = \tfrac{1}{2} \ln \left| \frac{1+z}{1-z} \right| + \begin{cases} \frac{1}{2}\mathrm{i}[\tan^{-1}(\delta_1) + \tan^{-1}(\delta_2)] & \lambda < 0 \\ -\frac{1}{2}\mathrm{i}[\tan^{-1}(-\delta_1) + \tan^{-1}(-\delta_2)] + \pi\mathrm{i} & \lambda > 0 \end{cases} \tag{28}$$

$$\delta_1 = \frac{z_i}{1+z_r} \qquad \delta_2 = \frac{z_i}{1-z_r} \qquad z = z_r + \mathrm{i}z_i = (s/\lambda)\,\mathrm{e}^{\mathrm{i}a}.$$

(ii) The infinite upper and lower bounds for the integrals $K_{mm'}$ of equation (18) can be truncated easily since, as $|\lambda| \to +\infty$, the integrand function vanishes as $\exp(-2|\lambda|D)$. A Simpson rule algorithm is adopted for the numerical computation of the integrals $K_{mm'}$.

4. Evaluation of the scattered field

Let us assume that the interior field $\psi(\boldsymbol{r})$ is known; then as a next step we consider the scattered field for $y > 0$. Substituting equation (13) into equation (12) and following an algebra similar to that of the previous section the field for the air region is obtained as

$$\psi(\boldsymbol{r}) = \psi_0(\boldsymbol{r}) + \sum_m \mathrm{i}^{-m} C_m L_m(X_1, X_2) Z_m(\boldsymbol{r}) \tag{29}$$

where

$$Z_m(\boldsymbol{r}) = \int_c \mathrm{d}\lambda \frac{\exp[-\mu_0(y-D) - \mu_1 D + \mathrm{i}\lambda x - \mathrm{i}m\theta_1]}{\mu_1 + \mu_0} \tag{30}$$

for $y > 0$. For the far field region it is possible to evaluate this integral using the steepest descent approximation. To this end transform the integration variable λ as

$$\lambda = -k_0 \cos\beta = -k_0 \cos\xi \cosh\eta + \mathrm{i}k_0 \sin\xi \sinh\eta$$

where $\beta = \xi + \mathrm{i}\eta$. Then the square root for μ_0 is defined as $\mu_0 = -k_0 \sin\beta$. This choice determines the regions of the β plane corresponding to the proper Riemann sheet of the β plane as shown in figure 4 (Collin 1960). Since μ_0 is an analytic function in the β plane no branch cuts are required for this function. The image of the branch cuts for the

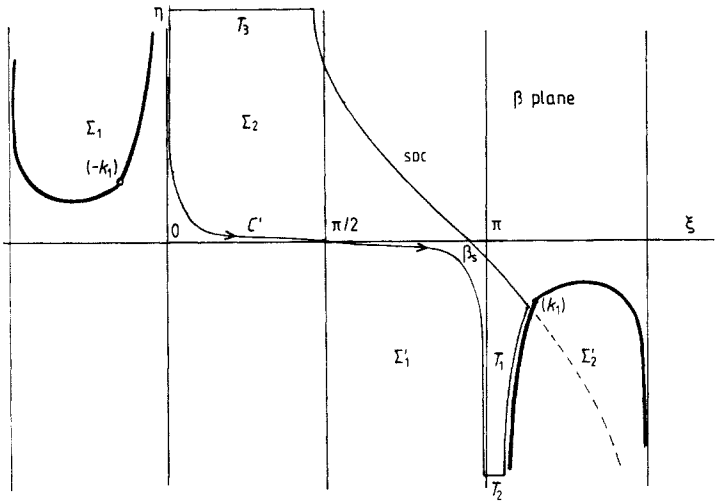

Figure 4. Steepest descent integration.

functions μ_1 and θ_1 in the β plane are shown in figure 4. The asymptotic values for the branch cuts $i\theta_1$, as $\eta \to \pm\infty$, are

$$\xi \to -T \qquad \text{as } \eta \to +\infty$$

and (31)

$$\xi \to \pi + T \qquad \text{as } \eta \to -\infty$$

where $\tan(T) = k_{1i}/k_{1r}$.

The transformation of the contour C of the λ plane is shown as C'. Following the standard procedure of the steepest descent approximation (Collin 1960, Jones 1964) the saddle points are determined to be

$$\frac{d}{d\beta}[k_0\rho \cos(\beta + \varphi)] = 0$$

or $\beta_s = \pi - \varphi$ and $-\varphi$, where $\varphi = \tan^{-1}(y/x)$ is the direction for which the field is evaluated. The steepest descent contours (SDC) passing through these saddle points are determined from the exponential function of the integrand of equation (30) and the condition (Collin 1960)

$$\text{Im}[i\lambda x - \mu_0 y - ik_0\rho \cos(\beta_s + \varphi)] = \text{Im}\{ik_0\rho[\cos(\beta + \varphi) - \cos(\beta_s + \varphi)]\} = 0$$

or

$$\cos(\xi + \varphi)\cosh(\eta) = \mp 1 \tag{32}$$

for $\beta_s = \pi - \varphi$ and $-\varphi$ respectively. Examination of the $\exp(i\lambda x - \mu_0 y)$ term of equation (30) shows that when $y > 0$ only the steepest descent path passing through the saddle point $\beta_s = \pi - \varphi$ can be used to close the contour C'. Proceeding further to the evaluation of the integral of equation (33), as a result of the Cauchy theorem we obtain

$$Z_m(\boldsymbol{r}) = \left(\int_{\text{SDC}} + \int_{T_1} + \int_{T_2} + \int_{T_3}\right) d\beta\, F_m(\beta) \tag{33}$$

where

$$F_m(\beta) = k_0 \sin\beta \frac{\exp(ik_0 \sin\beta y - ik_0 \cos\beta x)}{(k_0^2 \cos^2\beta - k_1^2)^{1/2} - ik_0 \sin\beta} \exp(-im\theta_1)$$
$$\times \exp\{-D[ik_0 \sin\beta + (k_0^2 \cos^2\beta - k_1^2)^{1/2}]\}. \tag{34}$$

T_1, T_2 and T_3 are defined as in figure 4. Note that if the contour SDC does not intersect the branch cuts for $i\theta_1$ or μ_1 the contribution from T_1 vanishes. This occurs when

$$\tfrac{1}{2}\pi - T < \varphi < \tfrac{1}{2}\pi + T. \tag{35}$$

It can be shown that the contribution of the contours T_1, T_2, T_3 vanishes as $|\eta| \to +\infty$ and $\rho = (x^2 + y^2)^{1/2} \to +\infty$ $(x \neq 0)$. Applying further the well known procedure for the

Table 1. Scattering coefficients for $\sigma_1 = 10^{-3}$ S m^{-1}, $\varepsilon_1/\varepsilon_0 = 4$, $\omega = 90°$ and 50 MHz frequency

m	$C_m^s(0)$	$C_m^s(1)$	$C_m^s(2)$
±1	−0.288 + 0.533i	0.511 + 0.803i	−0.740 + 1.36i
±1	0.288 − 0.533i	0.106 + 0.324i	0.232 − 0.322i
0	−0.288 + 0.533i	−0.715 − 0.125i	−0.299 − 0.383i

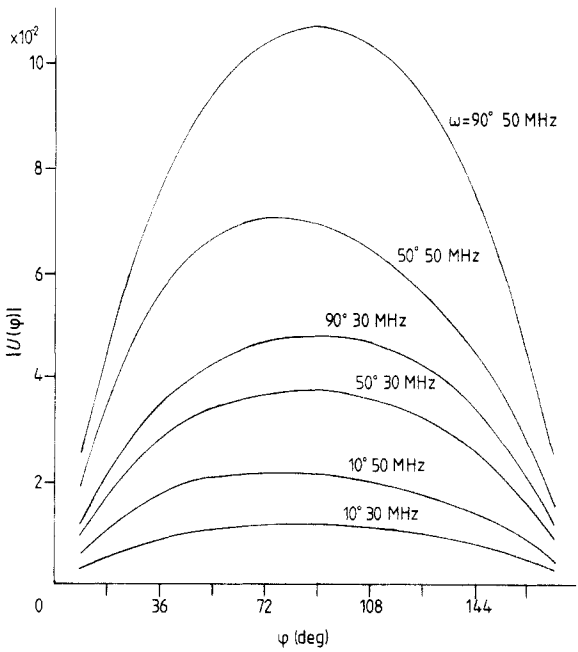

Figure 5. Scattering amplitude $|U(\varphi)|$ for various incident angles ω and 30 and 50 MHz radiation frequencies for ground with $\sigma_1 = 10^{-3}$ S m^{-1}, $\varepsilon_{r1} = 4$ and hollow cylindrical scatterers with $k_0 b = 0.5$, $k_0 D = 1$.

evaluation of the steepest descent approximation (Collin 1960) we finally obtain

$$Z_m(\boldsymbol{r}) = U_m(\varphi)\, e^{ik_0\rho}\left(\frac{2\pi}{k_0\rho}\right)^{1/2} e^{-i\pi/4} \tag{36}$$

where

$$U_m(\varphi) = k_0 \sin\varphi \frac{\exp\{-iD[k_0 \sin\varphi - i(k_0^2 \cos^2\varphi - k_1^2)^{1/2}]\}}{(k_0^2 \cos^2\varphi - k_1^2)^{1/2} - ik_0 \sin\varphi} \tag{37}$$

and $\theta_1(\beta_s)$ is computed from equation (28). Substitution of equation (36) into equation (29) determines the far field as

$$\psi \simeq \psi_0 + U(\varphi)\exp(ik_0\rho)\left(\frac{\pi}{2k_0\rho}\right)^{1/2} \tag{38}$$

where the scattering amplitude is defined as

$$U(\varphi) = 2e^{-i\pi/4} \sum_{m=-\infty}^{+\infty} i^{-m} C_m L_m(X_1, X_2) U_m(\pi - \varphi). \tag{39}$$

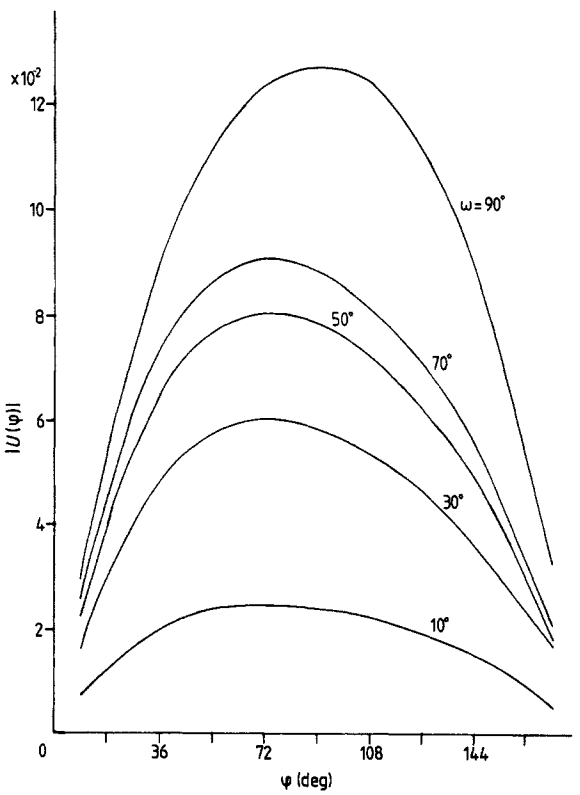

Figure 6. Scattering amplitude $|U(\varphi)|$ for 50 MHz with ground parameters $\sigma_1 = 10^{-3}$ S m^{-1}, $\varepsilon_{r1} = 4$, various incident angles ω and scatterer parameters $\sigma_2 = 10^{-2}$ S m^{-1}, $\varepsilon_{r2} = 3$, $D = 1$ m, $k_0 b = 0.5$.

5. Numerical results

Numerical computations have been performed using the results of §§ 3 and 4 when $|X_2 - X_1| < 1$. For each specific scatterer case the convergence of the expansion in equation (25) is verified. In table 1 results are given for the scattering coefficients $C_m(i)$ ($i = 0, 1, 2$) of a specific case. Numerical computations reveal that the number of partial waves to be taken into account, as in the free space scatterer case (Kerker 1969), is determined from the relative size parameter of the scatterer, i.e. $|X_2 - X_1|$. Since it is assumed that $|X_2 - X_1| < 1$, a small number of terms are sufficient to obtain convergence for the summation in equation (39).

In figure 5 results are given for the scattering amplitude $|U(\varphi)|$ of a hollow underground tunnel ($n_2 = 1$) for various incident angles ω and at 30 and 50 MHz frequencies. The scattering energy is concentrated towards the vertical ($\varphi \simeq 90°$) direction even for very small incident angles ω.

It should be noted that the presence of the lossy half-space medium destroys the conventional scattering pattern observed for free space scatterers. Instead of the well known Rayleigh scattering ($|X_2 - X_1| < 1$) pattern—with a maximum echo in the backward and forward directions—the maximum electromagnetic energy emerges following the shortest path inside the ground. In figure 6 the scattering amplitude is shown as a function of the scattering angle φ for a lossy scatterer with conductivity $\sigma_2 = 10^{-2}$ S m^{-1} and relative dielectric constant $\varepsilon_2/\varepsilon_0 = 3$ embedded inside the ground with $\sigma_1 = 10^{-3}$ S m^{-1} and $\varepsilon_1/\varepsilon_0 = 4$ at 50 MHz. The general characteristics of the scattering patterns are similar to the previous case.

The effect of scatterer depth is given in figure 7 where the scattering patterns are given for several depths (D) of a hollow cylinder. The expected exponential attenuation for the scattered wave is verified.

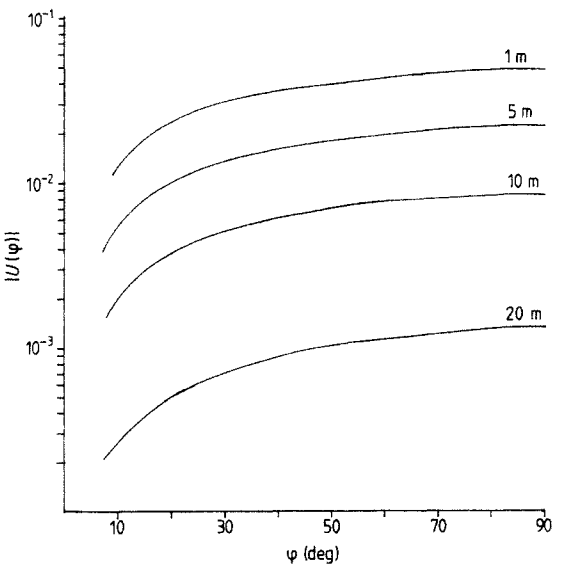

Figure 7. Scattering amplitude $|U(\varphi)|$ for various hollow scatterer axis depths D, $k_0 b = 0.5$, angle of incidence $\omega = 90°$ and radiation frequency 30 MHz.

6. Conclusions

An analytic procedure has been developed for the scattering of electromagnetic waves from underground cylindrical inhomogeneities. The case of small size $|X_2 - X_1| < 1$ scatterers was investigated in detail. In most practical cases this approximation is valid since the low-frequency side of the spectrum is usually employed for probing the ground environment. The analysis presents several analytical techniques that are necessary in the treatment of similar problems, i.e. scatterers inside a half-space lossy medium (see §§ 3 and 4). The scattered far field is computed in the air region by applying the steepest descent approximation technique. The maximum scattering energy is shown to be directed perpendicular to the ground surface almost independently of the value of the incidence angle. Finally it should be noted that a similar formulation can be used to treat problems such as three-dimensional scatterers and/or ground media with horizontally stratified layers.

Appendix. Expressions for $K_m(1)$, $K_m(2)$, $L_m(1)$, $L_m(2)$

Starting from the defining equations (23) and (24) for $j = 1, 2$ and applying the differentiation and recurrence relations among Bessel functions the following expressions are obtained:

$$K_m(1) = \pi i[m(H_m(x_1)J_{m+1}(x_1) + H_{m+1}(x_1)J_m(x_1)) - x_1(H_{m+1}(x_1)J_{m+1}(x_1) + H_m(x_1)J_m(x_1))] \tag{A1}$$

$$K_m(2) = -1 + \tfrac{1}{2}\pi i(J_{m+1}(x_1)H_{m+1}(x_1) - H_m(x_1)J_m(x_1)) - \frac{m}{x_1}\frac{\pi i}{2}\left(\frac{2im}{\pi x_1} + H_{m+1}(x_1)J_m(x_1) + J_{m+1}(x_1)H_m(x_1)\right) \tag{A2}$$

$$L_m(1) = x_1(J_m^2(x_1) + J_{m+1}^2(x_1)) - 2mJ_m(x_1)J_{m+1}(x_1) \tag{A3}$$

$$L_m(2) = \tfrac{1}{2}\left(J_m^2(x_1) - J_{m+1}^2(x_1) + \frac{2m}{x_1}J_m(x_1)J_{m+1}(x_1)\right). \tag{A4}$$

References

Abramowitz M and Stegun I A 1965 *Handbook of Mathematical Functions* (New York: Dover) p 484
Burrell G A and Peters L 1979 *Proc. IEEE* **67** 981–90
Cauterman M, Mertin J, Degauque P and Gabillard R 1979 *Proc. IEEE* **67** 1009–15
Chan L C, Moffatt D L and Peters L 1979 *Proc. IEEE* **67** 991–1000
Collin R E 1960 *Field Theory of Guided Waves* (New York: McGraw Hill) pp 486–95
Jones D S 1964 *The Theory of Electromagnetism* (Oxford: Pergamon) pp 438–50
Kerker M 1969 *The Scattering of Light* (New York: Academic) pp 104–27
Lee T 1979 *Prhc. IEEE* **67** 1016–21
Mahmoud S F, Botros A Z and Wait J R 1979 *Proc. IEEE* **67** 1022–9
Sommerfeld A R 1949 *Partial Differential Equations in Physics* (New York: Academic) pp 246–65
Sullivan W B 1970 *MSc thesis* Ohio State University
Tikhonv A N 1950 *Akad. Nauk. SSSR* **73** 295–7
Wait J R 1962 *J. Res. Nat. Bur. Stand.* D **66** 509–41